High Density EOS — Heavy-Ion Collisions, Compact Stars and Strangeness —

Akira Ohnishi[1]

[1]*Yukawa Institute for Theoretical Physics, Kyoto University, Kyoto 606-8502, Japan*

E-mail: ohnishi@yukawa.kyoto-u.ac.jp

(Received June 20, 2017; Revised August 8, 2017)

High density nuclear matter equation of state (EOS) is discussed. We first discuss that the recently observed negative slope of the proton directed flow requires softening of EOS at high density. We next give a brief review on possible solutions of the hyperon puzzle, three-baryon interactions, transition to quark matter, and modified gravity.

KEYWORDS: Directed flow, Softening, Hyperon puzzle

1. Introduction

The baryon density in the cores of massive neutron stars may reach $(4-10)\rho_0$, which is the largest density in stable matter in our universe. Because of the large chemical potential, various forms of matter are expected to appear in neutron star cores, such as strange hadrons, meson condensate, quark matter, and color superconductor, in addition to nucleons and leptons. It is also possible to probe various phases of nuclear matter by using heavy-ion collisions. At collider energies (RHIC and LHC), the quark gluon plasma (QGP) is formed with almost zero baryon chemical potential, while we can probe baryon-rich region by using lower-energy heavy-ion collisions. Compared with compact stars, the isospin asymmetry ($\delta = (N-Z)/A$) is small in heavy-ion collisions. At high temperatures, $T > 100$ MeV, pions are produced abundantly and reduce the anisotropy of baryonic part. Isospin chemical potential ($\delta\mu = \mu_n - \mu_p$) is evaluated to be 10 MeV or less in high-energy heavy-ion collisions, while it can reach $100-200$ MeV in neutron star matter. In order to understand the whole phase-diagram structure in (T, ρ_B, δ) space schematically shown in Fig. 1, we need to combine knowledge from compact stars and heavy-ion collisions.

One of the most interesting questions in dense nuclear matter physics is the existence of the first-order phase-transition boundary at high baryon densities. If the QCD phase transition in cold nuclear matter is of the first order, we must have at least one QCD critical point (CP) in the QCD phase diagram: The transition at zero baryon chemical potential is crossover, then the first-order phase boundary needs to terminate at CP. The existence of CP or the first-order phase transition boundary would be accessible in heavy-ion collisions. On the one hand, large fluctuations of conserved charges are expected around CP. Because of the second-order phase transition nature at CP, the susceptibilities and higher-order cumulants diverge at CP owing to the divergent correlation length, and thus one expects anomalously large fluctuations would be observed if the system passes around CP. Recent data show non-monotonic behavior of the fourth order cumulant ($\kappa\sigma^2$) of net proton numbers as a function of the colliding energy [1], and the interpretation of the data is under active debate. On the other hand, the softening of equation of state (EOS) is expected with the first-order phase transition, and causes reduction of the directed flow. The transverse collective flows, such as the directed flow $v_1 = \langle \cos\phi \rangle$ and the elliptic flow $v_2 = \langle \cos 2\phi \rangle$, have been utilized to explore the properties of hot and dense matter EOS in the early stages of heavy-ion collisions. Particles are generally kicked in the

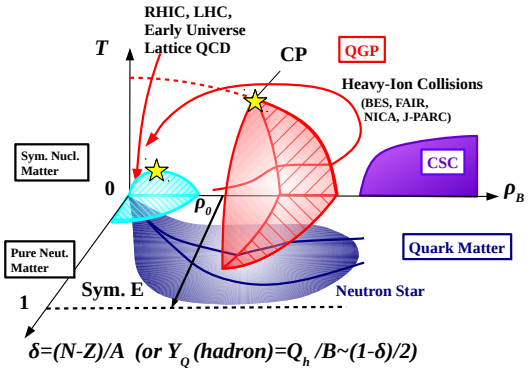

Fig. 1. Expected QCD phase diagram in the temperature (T), baryon density (ρ_B), isospin asymmetry (δ) space.

transverse direction by the hot and dense region having larger pressure, and the v_1 generally shows a positive slope as a function of rapidity, $dv_1/dy > 0$. When matter passes through the softening region, however, the negative slope of v_1 emerges as a consequence of a tilted ellipsoid with respect to the beam axis. Recent data show negative slope of proton v_1 at $\sqrt{s_{NN}} > 10$ GeV [2]. Thus the observed negative slope seems to suggest the softening of EOS, while its interpretation needs careful analysis of the EOS and dynamics.

Another important problem in dense matter physics is so-called the hyperon puzzle. The baryon density in neutron stars may reach $(4-10)\rho_0$, where the admixture of hyperons is expected from laboratory hypernuclear data combined with microscopic calculations starting from the NN and YN interactions as well as phenomenological calculations. Hyperons also cause the softening of EOS, and many of the hyperonic matter EOS cannot sustain massive neutron stars, $M \simeq 2M_\odot$ [3]. This inconsistency is called the hyperon puzzle. The hyperon puzzle is not only a problem in neutron star physics, but is also related with supernova (SN) explosions, dynamical black hole (BH) formations, and binary neutron star mergers (BNSM). In these compact star phenomena, the maximum densities are evaluated as $(2-3)\rho_0$ (SN [4]) and $\sim 10\rho_0$ (BH [5] and BNSM [6]), and the temperatures cannot be ignored. The density and temperature region of hyperon admixture may not be reached in neutron stars but can be accessible during the dynamical BH formation processes [6] or in the hyper massive neutron stars formed in the last stage of BNSM.

In this proceedings, we first discuss the EOS softening suggested by the recent data. Next, we discuss the possible solutions of the hyperon puzzle.

2. EOS softening probed in heavy-ion collisions

2.1 QCD phase transition signals in heavy-ion collisions

The properties of hot matter at small baryon density have been extensively investigated experimentally and theoretically. Theoretical arguments and circumstantial experimental evidence suggest that matter produced in heavy-ion collisions at RHIC and LHC energies is a QGP. The lattice QCD Monte-Carlo simulation is also available at zero baryon density, and shows that the transition is crossover. The discovery of QGP and its strongly interacting nature have opened a new area of research, partonic matter physics under extreme conditions.

One of the next grand challenges is the detection of the QCD phase transition: the first-order boundary or the second-order feature at CP. Detecting the phase transition in heavy-ion collisions is not an easy task because of the non-uniform and non-equilibrium features. Nevertheless, we already know one example of the observed first-order phase transition in nuclear matter, the liquid-gas

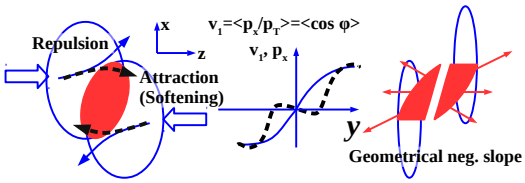

Fig. 2. Schematic picture of how the directed flow is generated. Left panel shows how particles are bended in the denser region when the EOS is softened. Right panel shows the geometrical mechanism to generate negative slopes.

phase transition. The temperature as a function of the energy per nucleon (caloric curve) [7] is obtained by using the double ratio of isotope yields, $(^7\mathrm{Li}/^6\mathrm{Li})/(^4\mathrm{He}/^3\mathrm{He})$. The caloric curve shows an approximate plateau of T, a clear signal of the first-order phase transition.

The QCD phase transition signal in heavy-ion collisions is not yet clear. By fitting the hadron yield ratio, the temperatures T and baryon chemical potentials μ_B are obtained and show decreasing T as a function of μ_B [8], as expected from the phase boundary in chiral effective models. However, the obtained "boundary" (μ_B, T) is believed to be the one at chemical freeze out, not at the QCD phase transition boundary. At colliding energies of $\sqrt{s_{NN}} = (5-20)$ GeV, non-monotonic behavior is observed in several observables [9], such as the K^+/π^+ ratio (horn), m_T slope parameter (step or re-hardening), and the rapidity distribution width of π (dale). While there are arguments on the relevance of these signals to the phase transition, fully consistent understanding is not obtained yet.

Recent observation of the non-monotonic dependence on the colliding energies in the cumulant of net-proton numbers [1] and the proton directed flow slope [2] seems to show clearer signals, as mentioned in the introduction. These observables are (more or less) directly related to the critical behavior around CP and the EOS softening. The cumulants of conserved charges should contain information across the phase boundary provided that the diffusion of conserved charges is not strong, and the momentum anisotropy produced in the early stages should survive even though later stage dynamics weakens the strength.

2.2 Negative directed flow

Now let us focus on the directed flow. The directed flow shows the first moment of the anisotropy in the particle distribution; $v_1(y) = \langle \cos\phi \rangle_y$ or $\langle p_x \rangle_y$, where the beam (impact parameter) is in the z (x) direction, ϕ is the azimuthal angle, and y denotes the rapidity. When the EOS is repulsive, forward-(backward-)going particles are kicked in the $+x$ $(-x)$ direction and the v_1 slope is positive, $dv_1/dy > 0$. The directed flow at colliding eneriges of $(1-11)A$ GeV (2 GeV $< \sqrt{s_{NN}} <$ 5 GeV) has been utilized to determine the stiffness of the EOS [10, 11]. When the EOS is softened by some mechanism, particles are bended in the denser direction as shown in the left panel of Fig. 2, and the directed flow can have a negative slope. Actually, the slope is predicted to show a minimum at a certain colliding energy in hydrodynamical calculations using an EOS with a first-order phase transition [12]. The negative slope has been predicted in microscopic hadron transport models at sufficiently high energies $\sqrt{s_{NN}} > 20$ GeV and at large impact parameters [13, 14], but the origin of the sign change is purely geometrical and is not related to the EOS softening, as shown in the right panel of Fig. 2. At higher energies, the interaction time becomes shorter, nucleons in the projectile and target nuclei go through each other, and the Bjorken picture rather than the Landau picture becomes valid. Nucleons in the projectile and target nuclei are slowed down according to the thickness of the reaction region. After passing through, particles are emitted in the outer region, and negative slope appears [13]. Thus the Bjorken picture and the dominance of the later stage repulsion generate the negative slope at $\sqrt{s_{NN}} > 20$ GeV.

Recently the directed flows of protons, anti-protons, pions and kaons are observed in the beam

energy scan (BES) program at RHIC [2]. The collapse of the proton directed flow slope to a negative value is observed at $\sqrt{s_{NN}} > 10$ GeV. This collapse energy is higher than that in the old hydrodynamics predictions and lower than that of the geometrical slope change predicted in hadronic transport models. Then it might signal the softening of EOS.

The excitation function of the directed flow slope has been investigated also with EOS softening effects, but the conclusions are controversial. Strong EOS sensitivities of the directed flow slope are found in a three-fluid model, which indicates that the crossover EOS is consistent with the directed flow data of energy range up to $\sqrt{s_{NN}} = 11.5$ GeV [15]. In a transport model calculation with a first-order phase-transition EOS, a negative slope is found to appear but at a lower colliding energy [16]. By comparison, in a transport+hydrodynamics hybrid approach, the directed flow is found to be insensitive to the EOS, and there is no minimum in the excitation function of the directed flow slope [17]. In the PHSD transport model which incorporates crossover EOS, the collapse energy is found to be higher and the experimentally observed minimum does not appear [14]. Thus it is not yet clear whether the negative slope of v_1 signals the softening of the EOS in hybrid approaches.

2.3 Hadronic transport model analyses of directed flow

For the analyses of heavy-ion collisions in the colliding energy range of $\sqrt{s_{NN}} = (5 - 20)$ GeV, complete thermalization cannot be expected and we should invoke non-equilibrium dynamics such as the transport model approaches or hybrid approaches. Here we analyze the directed flow by using the hadronic cascade model JAM [18] with and without the EOS softening effects.

We first examine the standard hadronic transport model results of the directed flow. In the left panel of Fig. 3, we show the calculated directed flow v_1 of protons and pions as functions of rapidity in mid-central collisions in the cascade model JAM (dotted lines) in Au+Au collisions at $\sqrt{s_{NN}} = 7.7, 11.5, 19.6$ and 27 GeV [20] in comparison with the STAR data [2]. While the cascade results agree with the 7.7 GeV data, v_1 from the standard cascade for beam energies of 11.5 and 19.6 GeV yields much larger v_1 slope than the data. The proton v_1 slope at $\sqrt{s_{NN}} = 27$ GeV and pion v_1 slopes are negative in the standard cascade from geometrical non-QGP effects [13] and from absorption by baryons [21], respectively.

Next we examine the nuclear mean field effects. Skyrme-type density dependent and Lorentzian-type momentum dependent nuclear mean field of baryons are included based on the framework of simplified version of relativistic quantum molecular dynamics (RQMD/S) in Ref. [11], but with slightly different parameter sets which yields the incompressibility of $K = 272$ MeV [22]. The hadronic transport model with momentum dependent mean field describes the directed flow data in the corresponding energy region better [11, 19]. The mean field slightly reduces the proton directed flow at $\sqrt{s_{NN}} = 11.5$ GeV, but the basic trend is the same as the cascade, and does not explain the negative slope of proton v_1 as shown in the top right panel of Fig. 3 [20]. Even if we modify the mean field treatments, there is no qualitative differences. Thus we conclude that hadronic transport models with standard cascade do not explain the negative v_1 slope of protons at 11.5 and 19.6 GeV.

2.4 EOS softening effects

We shall now examine the EOS softening effects. We take into account nuclear EOS effects in the hadronic transport model JAM by changing the stochastic two-body scattering style [23–25], which is normally implemented so as not to contribute to the pressure. By this way of effective EOS modification, we can simulate a variety of EOS by switching off and on the attractive orbits, then it is found to be very useful [20]. By imposing attractive orbits for each two-body hadron-hadron scattering, the pressure is reduced as given by the virial theorem [25]. In interacting many-particle systems, the pressure is obtained as the derivative of the virial G,

$$G \equiv \sum_i \boldsymbol{r}_i \cdot \boldsymbol{p}_i \,, \quad P = \frac{1}{3V}\frac{dG}{dt} = \frac{1}{3V}\sum_i \left[\boldsymbol{v}_i \cdot \boldsymbol{p}_i + \boldsymbol{r}_i \cdot \frac{d\boldsymbol{p}_i}{dt} \right] . \tag{1}$$

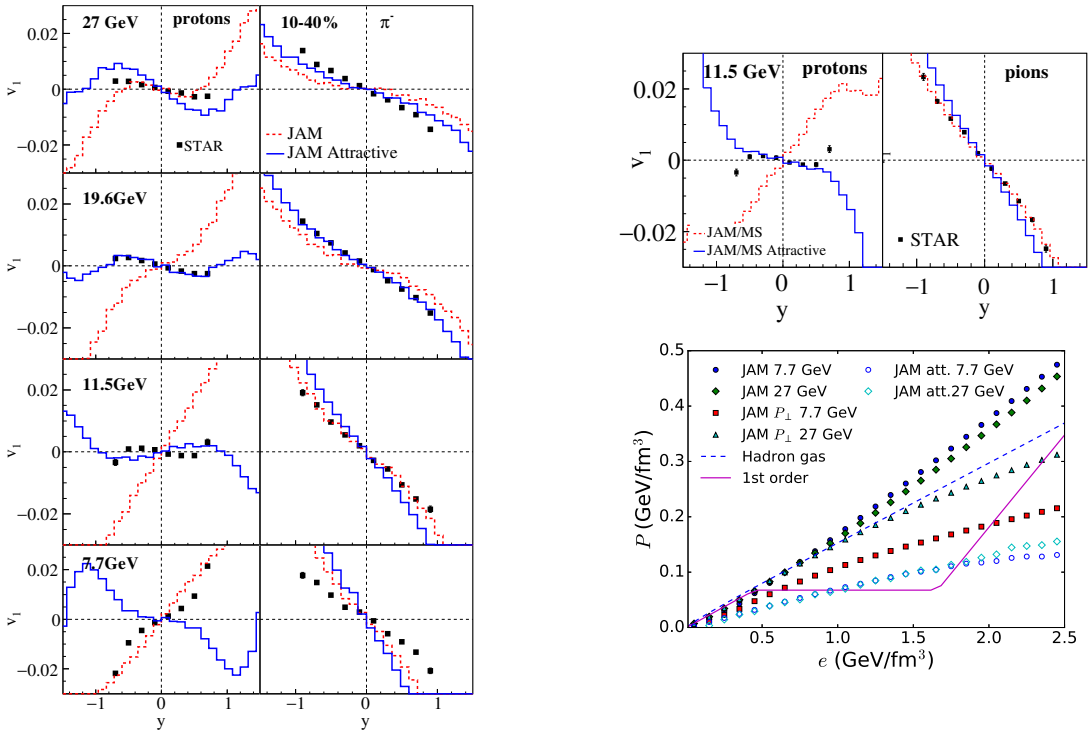

Fig. 3. Left: Directed flows of protons and pions in mid-central Au+Au collisions (10-40%) at $\sqrt{s_{NN}}$ = 7.7-27 GeV from the standard cascade (dashed lines) and the cascade with attractive orbits (solid lines) in comparison with the STAR data [2]. Top right: Directed flows calculated with momentum dependent hadronic mean-field potentials (JAM/MS) at $\sqrt{s_{NN}}$ = 11.5 GeV. Solid and dashed lines show results of JAM/MS in the standard and attractive orbit modes, respectively. Bottom right: Effective EOS extracted from the time evolution of simulations in Au+Au collisions at $\sqrt{s_{NN}}$ = 7.7 and 27 GeV. Full (open) circles and diamonds represent the pressures P from standard JAM (JAM with attractive orbits) at 7.7 and 27 GeV, respectively. The dashed and sold lines represent the EOS from hadron gas and the EOS with a first-order phase transition used in Ref. [26]. Taken from Ref. [20].

When there is no potential effects, the momentum change $d\boldsymbol{p}_i/dt$ is caused by the particle collisions,

$$P = P_f + \frac{1}{3V\Delta t}\sum_{(i,j)} \boldsymbol{q}_{ij}\cdot\left(\boldsymbol{r}_i - \boldsymbol{r}_j\right) \tag{2}$$

where $P_f = \int dt \sum_i \boldsymbol{p}_i\cdot\boldsymbol{v}_i/(3V\Delta t)$ corresponds to the kinetic contribution. The second term represents the pressure from two-body scatterings, where $\boldsymbol{q}_{ij} = \boldsymbol{p}'_i - \boldsymbol{p}_i = -(\boldsymbol{p}'_j - \boldsymbol{p}_j)$ is the momentum transfer and $\boldsymbol{r}_i$ and $\boldsymbol{r}_j$ are the coordinates of colliding particles i and j, respectively. V is the volume of the system, and Δt is a time interval over which the system is measured. Thus, repulsive orbits $\boldsymbol{q}_{ij}\cdot(\boldsymbol{r}_i - \boldsymbol{r}_j) > 0$ enhance the pressure, while attractive orbits $\boldsymbol{q}_{ij}\cdot(\boldsymbol{r}_i - \boldsymbol{r}_j) < 0$ reduce the pressure. Attractive orbits are implemented in the simulation by exchanging the momentum of two particles in the two-body center-of-mass (c.m.) frame when the randomly chosen scattering orbit is repulsive. While in reality softening of EOS should depend on the local energy density and temperature, we impose a modified scattering style for all hadron-hadron $2 \to 2$ scatterings in order to examine the softening effects.

In the left panel of Fig.3, we show the results with the EOS softening effects. Compared with the standard cascade results, attractive orbits drastically reduce the v_1 slope, and explain the STAR data at $\sqrt{s_{NN}} \gtrsim 10$ GeV. Particularly, the v_1 slope becomes almost zero and negative at $\sqrt{s_{NN}}$ = 11.5 and 19.6 GeV, respectively. We note that attractive orbits supplemented by the mean field yields negative

slope of proton v_1 at $\sqrt{s_{NN}} = 11.5$ GeV, as shown in the top right panel of Fig. 3. At lower energy $\sqrt{s_{NN}} = 7.7$ GeV, results with attractive orbits are far from the data. It is interesting to find that JAM results with attractive orbits overestimates the negative slope of the proton v_1 at $\sqrt{s_{NN}} = 27$ GeV, indicating the need of EOS rehardening, i.e. created matter at this colliding energy reaches well above the transition region or less net baryonic density leads to weaker softening of the EOS.

The EOS softening by attractive orbits is quantified by the pressure generated by a two-body collision obtained by using the formula [24],

$$\Delta P = -\frac{\rho}{3(\delta\tau_i + \delta\tau_j)} q^{\mu}_{ij}(x_i - x_j)_{\mu} \,, \tag{3}$$

where x_i is the space-time coordinate of particle i, q_{ij} is the four-momentum transfer, ρ is the Lorentz invariant local particle density, and $\delta\tau_i$ is the proper time interval between successive collisions. In the bottom right panel of Fig. 3, we show the "effective EOS" obtained by using the local pressure $P = P_f + \Delta P$ and energy density e at each collision point in the central region [20] in comparison with the ideal hadron gas EOS and the EOS with a first-order phase transition (EOS-Q) [26]. With attractive orbits, we see a significant reduction of the pressure, which is comparable in strength to EOS-Q in the transition region.

3. Compact star matter EOS and Strangeness

After the discovery of massive neutron stars with $M \simeq 2M_{\odot}$, the hyperon puzzle has been attracting much attention. Many of the hyperonic matter EOSs are constructed based on hypernuclear physics information, (1) Λ potential in nuclear matter is around $U_{\Lambda} \sim 30$ MeV at ρ_0, (2) Σ potential in symmetric nuclear matter is repulsive, $U_{\Sigma} > +20$ MeV at ρ_0, and (3) Ξ potential is weakly attractive, $U_{\Xi} \simeq -14$ MeV at ρ_0. One also usually assumes (4) coupling constants of hyperons with vector mesons is given by the quark number counting rule, $g_{\omega\Lambda} \simeq g_{\omega\Sigma} \simeq 2g_{\omega\Xi} \simeq 2g_{\omega N}/3$, in relativistic mean field models, or (5) the three-baryon (3B) interaction involving hyperons is small and/or weaker than NNN interaction. Recent hypernuclear physics experiments have confirmed the point (2) and (3). The production spectrum in ${}^{6}\mathrm{Li}(\pi^-, K^+)\Sigma^{-5}\mathrm{He}$ reaction [27] is found to be consistent with $U_{\Sigma} \simeq +30$ MeV [28], and the newly discovered Ξ bound state of Ξ^--${}^{14}\mathrm{N}$ [29] suggests attractive nature of the ΞN interaction. Then we have to doubt the assumptions of (4) or (5) in hadronic matter scenario.

Several mechanisms have been proposed so far to solve the hyperon puzzle. In the first category of solutions, one introduces 3B repulsion or density dependence in the two-baryon interaction [30–32]. In the second category of solutions, quark matter core is assumed [33, 34]. The third way is to invoke the modified gravity [36].

In the quark matter scenario, if the QCD phase transition at high densities is of the first order, EOS is generally softened and hadronic EOS needs to be stiff enough to support $2M_{\odot}$ neutron stars. One of the ideas to avoid this softening is to consider the crossover transition [33] from nuclear matter to quark matter takes place at relatively low density, $(2-3)\rho_0$, instead of the first-order QCD phase transition at high density. In this case, the crossover transition may occur at lower density than the onset of hyperon mixing, and one can avoid the EOS softening from hyperons as well as the first-order phase transition. If the EOS is stiffened at high density in neutron star matter and is softened at high density in almost symmetric nuclear matter as suggested by the directed flow collapse, nuclear symmetry energy needs to be very large at high densities or the softening needs to start at higher density than the neutron star core. The directed flow analysis suggests that the softening starts at around $5\rho_0$ [20], then there is no contradiction if the neutron star core density is below $5\rho_0$.

The 3B repulsions or density dependence of two-baryon interactions have been investigated extensively [30–32]. While the 3B interaction effects on finite nuclei are not large, one can constrain its strength by using heavy-ion scattering, from the chiral effective field theory, from the lattice cal-

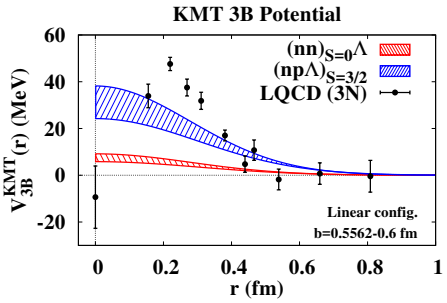

Fig. 4. Three-baryon potential in $(nn)_{S=0}\Lambda$ and $(np\Lambda)_{S=3/2}$ channels generated by the determinant interaction [32]. Shaded area shows the uncertainties from the size parameter. Filled circles show the results of the $3N$ potential obtained in the lattice QCD simulation [31].

culation, or by the quark model. Recent studies suggest that 3B interactions involving hyperons are as repulsive as or more repulsive than the three-nucleon interaction. In Fig. 4, we show the $NN\Lambda$ interaction from the determinant three-quark interaction [32]. The determinant interaction acts as a repulsive three-quark interaction among u, d and s quarks, and gives rise to YNN, YYN and YYY repulsion. This repulsion is comparable in strength with the NNN interaction obtained in the lattice QCD calculation [31]. As a result of comparable or more repulsive 3B repulsion in channels including hyperons, hyperon potential in nuclear matter saturates at around ρ_0, becomes shallower or repulsive above ρ_0. This early "turn over" from $dU_\Lambda/d\rho_B < 0$ to $dU_\Lambda/d\rho_B > 0$ may be the mechanism to delay or suppress the hyperons to appear in neutron star matter. In order to confirm the strength of the 3B interaction, we may need precise few-body hypernuclear data and/or precise Λ separation energy and its mass dependence.

It should be noted that the bare 3B interactions from lattice QCD or the determinant interaction shown above are much smaller than phenomenological 3B interactions. Then the main part of the 3B repulsion in nuclear matter should come from the generated 3B interaction. For example, the Pauli blocking in the intermediate state strongly suppresses the attraction from two-pion exchange processes, and this suppression plays the role of 3B repulsion or the density-dependent repulsion.

4. Summary and discussion

In this proceedings, we have discussed the high density EOS, focusing on the EOS softening suggested by recent direct flow measurement and the hyperon puzzle. Dense matter EOS is important in nuclear physics and astrophysics. In compact star phenomena (neutron stars, supernovae, black hole formation, binary neutron star mergers), very dense matter would be created, and non-nucleonic hadrons and quarks may emerge. In heavy-ion collisions at $\sqrt{s_{NN}} = (5 - 20)$ GeV, very dense (and partially equilibrated) matter would be formed. Recent observation of the directed flow collapse ($dv_1/dy < 0$) seems to indicate softening of the EOS at high densities. Existence of massive neutron stars imply stiff EOS in isospin asymmetric dense matter, and requires some mechanism such as three-baryon repulsive interaction, transition to quark matter, or modified gravity. Consistent understanding of heavy-ion collisions and compact stars would be helpful to draw the QCD phase diagram in the three-dimensional space, (T, μ_B, δ).

This work was supported in part by KAKENHI from JSPS and MEXT (Nos. JP15K05079, JP15H03663, JP15K05098, JP24105001 and JP24105008).

References

[1] L. Adamczyk et al. [STAR Collaboration], Phys. Rev. Lett. **112**, 032302 (2014).
[2] L. Adamczyk *et al.* [STAR Collaboration], Phys. Rev. Lett. **112**, 162301 (2014).
[3] P. Demorest et al., Nature, **467**, 1081 (2010); J. Antoniadis et al., Science, **340**, 6131 (2013).
[4] K. Sumiyoshi et al., Astrophys. J. **629**, 922 (2005); C. Ishizuka et al., J. Phys. G **35**, 085201 (2008);
[5] K. Sumiyoshi et al., Phys. Rev. Lett. **97**, 091101 (2006); Astrophys. J. **690**, L43 (2009); E. O'Connor and C. D. Ott, Astrophys. J. **730**, 70 (2011); A. Ohnishi et al., Phys. Lett. B **704**, 284 (2011); K. Nakazato et al., Astrophys. J. **745**, 197 (2012).
[6] K. Hotokezaka *et al.*, Phys. Rev. **D87**, 024001 (2013); Phys. Rev. **D88**, 044026 (2013); M. Hanauske *et al.*, Phys. Rev. D **96**, 043004 (2017).
[7] J. Pochadzalla et al. (GSI-ALLADIN collab.), Phys. Rev. Lett. **75**, 1040 (1995).
[8] A. Andronic, P. Braun-Munzinger and J. Stachel, Nucl. Phys. A **772**, 167 (2006).
[9] A. Rustamov, Central Eur. J. Phys. **10**, 1267 (2012).
[10] P. K. Sahu et al., Nucl. Phys. A **672**, 376 (2000); P. Danielewicz et al., Science **298**, 1592 (2002).
[11] M. Isse, A. Ohnishi, N. Otuka, P. K. Sahu and Y. Nara, Phys. Rev. **C72**, 064908 (2005).
[12] D. H. Rischke *et al.*, Heavy Ion Phys. **1**, 309 (1995); L. P. Csernai and D. Rohrich, Phys. Lett. **B458**, 454 (1999); J. Brachmann *et al.*, Phys. Rev. **C61**, 024909 (2000); Y. B. Ivanov *et al.*, Heavy Ion Phys. **15**, 117 (2002); V. D. Toneev *et al.*, Eur. Phys. J. **C32**, 399 (2003).
[13] R. J. M. Snellings, H. Sorge, S. A. Voloshin, F. Q. Wang and N. Xu, Phys. Rev. Lett. **84**, 2803 (2000).
[14] V. P. Konchakovski, W. Cassing, Y. B. Ivanov and V. D. Toneev, Phys. Rev. **C90**, 014903 (2014).
[15] Y. B. Ivanov and A. A. Soldatov, Phys. Rev. C **91**, 024915 (2015).
[16] B. A. Li and C. M. Ko, Phys. Rev. C **58**, R1382 (1998).
[17] J. Steinheimer, J. Auvinen, H. Petersen, M. Bleicher and H. Stcker, Phys. Rev. C **89**, 054913 (2014).
[18] Y. Nara, N. Otuka, A. Ohnishi, K. Niita and S. Chiba, Phys. Rev. **C61**, 024901 (2000).
[19] H. Liu *et al.* [E895 Collaboration], Phys. Rev. Lett. **84**, 5488 (2000); H. Appelshauser *et al.* [NA49 Collaboration], Phys. Rev. Lett. **80**, 4136 (1998); C. Alt *et al.* [NA49 Collaboration], Phys. Rev. **C68**, 034903 (2003).
[20] Y. Nara, H. Niemi, A. Ohnishi and H. Stcker, Phys. Rev. **C94**, 034906 (2016).
[21] S. A. Bass, C. Hartnack, H. Stoecker and W. Greiner, Phys. Rev. **C51**, 3343 (1995).
[22] Y. Nara and A. Ohnishi, Nucl. Phys. **A956**, 284 (2016).
[23] E. C. Halbert, Phys. Rev. **C23**, 295 (1981); M. Gyulassy, K. A. Frankel and H. Stoecker, Phys. Lett. **B110**, 185 (1982); D. E. Kahana *et al.*, Phys. Rev. Lett. **74**, 4404 (1995); Phys. Rev. **C56**, 481 (1997).
[24] H. Sorge, Phys. Rev. Lett. **82**, 2048 (1999).
[25] P. Danielewicz and S. Pratt, Phys. Rev. **C53**, 249 (1996).
[26] P. F. Kolb *et al.*, Phys. Lett. **B459**, 667 (1999); Phys. Rev. **C62**, 054909 (2000); H. Song and U. W. Heinz, Phys. Rev. **C77**, 064901 (2008).
[27] H. Sugimura *et al.* [J-PARC E10 Collaboration], Phys. Lett. B **729**, 39 (2014); R. Honda *et al.*, Phys. Rev. C **96**, 014005 (2017).
[28] T. Harada et al., in prep.
[29] K. Nakazawa *et al.*, Prog. Theor. Exp. Phys. **2015**, 033D02 (2015).
[30] S. Nishizaki et al., Prog. Theor. Phys. **108**, 703 (2002); Y. Yamamoto et al., Phys. Rev. C **90**, 045805 (2014); H. Togashi et al., Phys. Rev. C **93**, 035808 (2016); D. Lonardoni et al., Phys. Rev. C **89**, 014314 (2014); Phys. Rev. Lett., **114**, 092301 (2015); J. Rikovska-Stone et al., Nucl. Phys. A **792**, 341 (2007); T. Miyatsu et al., Astrophys. J. **777**, 4 (2013); S. Petschauer et al., Phys. Rev. C **93**, 014001 (2016); M. Kohno, Phys. Rev. C **88**, 064005 (2013).
[31] T. Doi et al., Prog. Theor. Phys. **127**, 723 (2012).
[32] A. Ohnishi, K. Kashiwa, K. Morita, Prog. Theor. Exp. Phys. **2017**, 073D04 (2017).
[33] K. Masuda, T. Hatsuda, and T. Takatsuka, Astrophys. J. **764**, 12 (2013); Prog. Theor. Exp. Phys. **2013**, 073D01 (2013).
[34] L. Bonanno, A. Sedrakian, Astron. Astrophys. **539**, A16 (2012); R. Lastowiecki et al., Acta Phys. Polon. Supp. **5**, 535 (2012).
[35] M. Kobayashi and T. Maskawa, Prog. Theor. Phys. **44**, 1422 (1970); M. Kobayashi, H. Kondo, and T. Maskawa, Prog. Theor. Phys. **45**, 1955 (1971); G. 't Hooft, Phys. Rev. D **14**, 3432 (1976) [Erratum: Phys. Rev.D **18**, 2199 (1978)]; Phys. Rept., **142**, 357 (1986).
[36] A. V. Astashenok et al., Phys. Rev. D **89**, 103509 (2014); M. K. Cheoun et al., J. Cosmol. Astropart. Phys. **1310**, 021 (2013).